Characterization of an Injection Molding Process for Improved Part Quality

A. Ghose, M. Montero, D. Odell
Berkeley Manufacturing Institute, Dept. of Mechanical Engineering
University of California - Berkeley

Abstract
An injection molding process was characterized with respect to certain physical characteristics of an injection molded part. The produced part, the "Triconnector", is a planar Lego-like piece, which was shot from ABS thermoplastic on a Morgan-Press G-100T Injection Molding Machine. Using statistical design of experiments, we identified the most significant parameters affecting part quality. The parameters used fell into three main categories: machine, process, and material. Part quality was defined by part fill, sink, and flash. Predictive models of part quality were developed and tested. It was found that ram speed, mold pre-heat, and nozzle temperature most affect part fill. Similarly, it was found that barrel temperature and cycle time most affect the sink of the sprue. A reliable predictive model for flash could not be developed, as there was too much variability in the results.

Keywords: Injection molding, Triconnector, Morgan Press, factorial design of experiments,

1 MOTIVATION

Injection molding is a time-saving and cost-effective means of producing, *en masse*, plastic parts. Hence, we proposed to characterize certain physical characteristics of injection molded parts as functions of parameters specific to the Morgan Press G-100T Injection Molding Machine. Our work was a natural follow-up of the development of an injection molding pipeline, for faster time-to-market products, in the Berkeley Manufacturing Institute. We could exploit the existing modules of the pipeline to design the mold from a manufacturability point-of-view, and machine the mold on an open architecture Haas VF-0 Milling Machine present in the same laboratory.

In selecting our experimental part, we were motivated by an idea conceived by Professor Carlo Sequin, of the Department of Computer Science, and aptly named the "Triconnector". It is analogous to a planar Lego-like building piece, with snap fits at the ends of its fingers, for easy creation of three-dimensional shape. For example, a dome can be created out of five of these interconnected parts, a flat surface out of six, and a saddle surface out of seven (Figure 20). Twenty of these connected parts, or four domes, would generate a sphere (Figure 21). We found this to be an attractive prospect for investigating the dependence of part fill, sink, and flash on the Morgan Press machine parameters.

2 TRICONNECTOR DESIGN

The Tri-Connector went through several iterations before the final design was settled upon. The part had to demonstrate that it met several criteria of design and manufacturability before the effort of creating a mold would be worthwhile.

To fulfil its design intent, the part had to snap together well with other parts, flex sufficiently to form the desired topology, and be symmetrical to insure that parts could snap together in any orientation (e.g. inverted). Design criteria were tested by creating part prototypes using the Fused Deposition Modeling (FDM) process (Figure 1).

In addition, there are many manufacturing requirements for the injection molding process that had to be addressed. In other words the part had to comply with the design for manufacturability (DFM) rules required for injection molding to be successfully molded. Some of these include the necessity of adding a sprue, runners, and gates to the part, as well as sizing and shaping the part appropriately. Of course, some of these criteria were in direct conflict with each other (such as flexibility, and sizing for molding). In addition to the molding criteria, the part had to be designed so that the mold could be machined on our in-house Haas VF-0 3-axis vertical mill. This limited the size of some of the features on the lower end.

Figure 1: FDM prototype of the Triconnector

Since the limits of the Morgan G-100T were known in advance, the part could be designed to function within these parameters. The biggest constraints of the Morgan G-100T are the maximum injection pressure (12,000 psi.), the clamp force (20 tons), and the fill volume (4 oz.). Since the triconnector is a relatively thin part, it requires relatively high injection pressures. Correspondingly, the clamp force (which is a function of injection pressure, material viscosity, and the projected area of the part) was relatively high. In this case, it turned out that the clamp force was the limiting factor.

Once a solid model was developed for the mold using SolidWorks 2000®, Moldflow's Cmold® software was used to simulate the injection process. The results of the final simulation are shown in Table 1 and Figure 2. However, to accommodate the Morgan G-100T's limits, several simulations and design iterations were required to arrive at these final values. A large factor was left between the simulation results and the press capabilities

as this simulation assumes a production mold and press, whereas a short-run mold and press were actually used.

Total part volume	0.24 in^3
Total part weight	0.15 oz
Total projected area	4.42 in^2
Average part thickness	0.05 in
Standard deviation of part thickness	0.02 in
Fill time	0.50 s
Packing/Holding time	1.73 s
Cooling time	6.47 s
Maximum injection pressure	3386.61 psi
Packing/Holding pressure	2709.29 psi
Melt temperature	500.00 F
Mold temperature	150.00 F
Required clamp force	5.99 ton(US)
Required shot size	0.15 oz

Table 1: Simulation Results

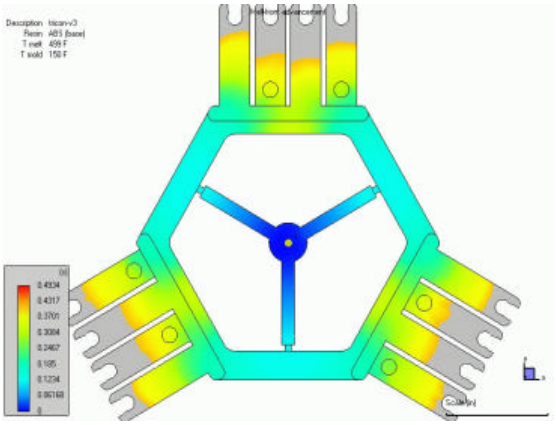

Figure 2: Simulation Results

Once the prototype verified the function of the part, and the simulation verified the viability of the mold, the design was considered complete. At this point, the mold was machined. The NC codes for the mold were generated using the automated process planner from the CyberCut pipeline. The input to the process planner was generated by exporting a .SAT file from the solid model of the mold design. These NC codes were then used to mill the mold halves. As the mold was to be used for small batch production, it was machined out of aluminium.

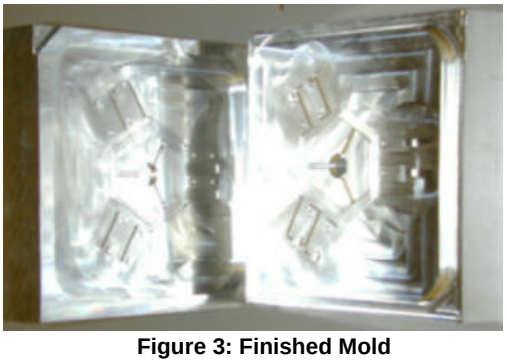

Figure 3: Finished Mold

Figure 3 shows a picture of the completed mold. After machining the mold, the cavity sections were hand finished using 220 grit sandpaper.

It is important to note that while the design and manufacture of the mold take up only a small portion of this paper, the majority of the project time was spent on it. This time investment was critical, as part design plays a huge factor in molded part quality. If this factor is not taken into account, fallible conclusions can be drawn from subsequent testing.

3 TESTING PROCEDURE

As previously mentioned, the tests were run on a Morgan G-100T injection press. Figure 4 shows this press, along with its notable features. More accurate digital temperature controls are included on the actual injection press, as opposed to the analog controls shown. In addition to temperature controls for the nozzle and barrel, the press has controls for: injection pressure, injection ram speed, clamp force, and mold pre-heat. The mold pre-heat plate brings the mold up to an elevated temperature to facilitate the flow of plastic through it. This prevents the material from solidifying too quickly and yielding in a short-shot. Injection ram speed controls the flow rate of plastic into the mold. The scale of the ram speed control on this press is relative (unitless). Nozzle and barrel temperature are self-descriptive terms, as is injection pressure. Cycle and cooling times are controlled by the injection and clamp control buttons. Since this was a short production run mold, part ejection was manual. All of these parameters were listed under the “machine“ heading of the fishbone diagram for the system response shown in Figure 5.

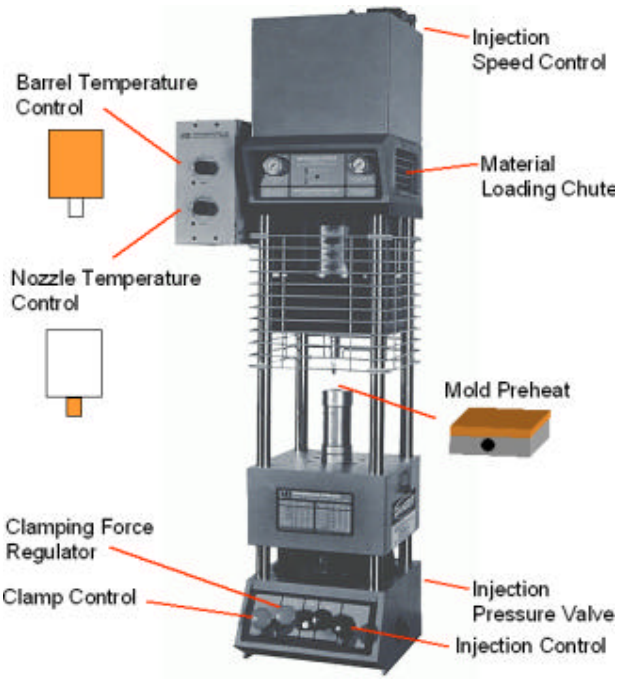

Figure 4: Morgan G-100T Injection Press

Under the fishbone category “material,” material type, material color, and material preparation were listed. Material preparation denotes the drying that is usually performed on polymers prior to molding. Drying is often required as many polymers are hydroscopic and will absorb moisture from the air over time. This can lead to superheated water bubbles forming in the material

potentially causing visual defects and unacceptable surface roughness.

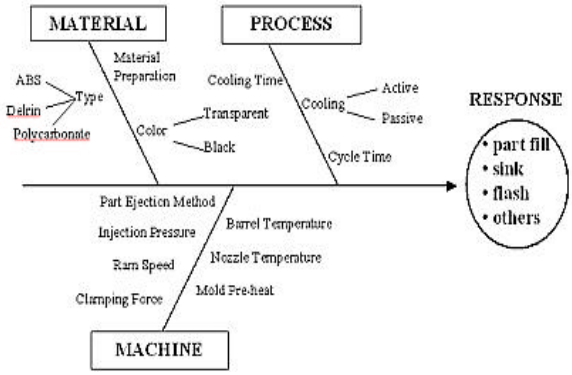

Figure 5: Fishbone Diagram of System Response

"Process" variables include cooling time, cooling method, and cycle time. We defined cycle time to include the total time required for injection and packing/holding. The pressure was set to be constant throughout this cycle (although there was some fluctuation due to the function of the press and the compressor). Cooling time was defined as the time the pressure was removed from the mold, but the clamp force remained. Some additional cooling would take place while the mold was removed from the press, and the part removed. However, it was impossible to control this additional time as the time to remove the part varied greatly due to the need for manual part ejection. For our experiment, a cooling time of 15 seconds was used. Passive cooling is simply exposing the mold to air. Active cooling is most commonly implemented by cutting channels into the mold and flowing cool water through them (similar to a radiator). Since this was a short run mold, and cycle time was not critical, passive cooling was considered ample.

Possible outputs for this system include: part fill, sink, flash, surface roughness, dimensional accuracy, stiffness (or other material properties) and visual defects. For this experiment, only part fill, sink, and flash were considered. Part fill describes how full the mold was when it was opened. Improper fill results in a "short shot," in which the part is only partially formed in the mold. See Figure 6 for a picture of part fill progression from extreme short shot to extreme flash. The left part on the bottom row represents an ideal part.

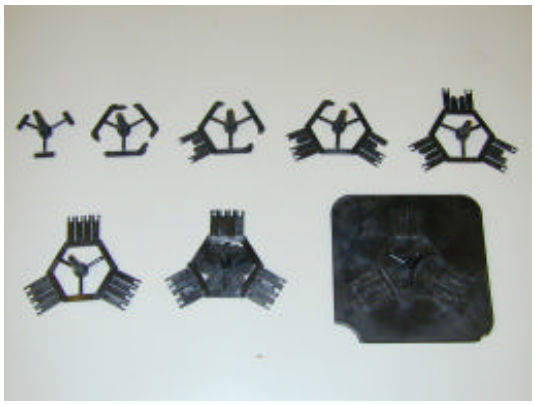

Figure 6: Mold Fill Progression

Flash occurs when extra material seeps out of the parting line of the part. This results in a thin layer of plastic hanging beyond the boundary of the part. It is generally considered to be caused by: excessive injection pressure, insufficient clamp force, or mold wear. If flash occurs, it must be hand trimmed, resulting in higher part cost. Figure 7 shows a close-up picture of flash at the end of one set of triconnector fingers.

Figure 7: Finger Flash

Sink is caused by non-uniform cooling in the part. As polymers cool from the molten state, they shrink. If a section of the part takes longer to cool, it will shrink more than the rest of the part. This typically occurs in thick sections, which have a higher volume to cooling surface area ratio. Sink results in reduced part performance, and visual defects. A picture of sink progression of the sprue is provided in Figure 8.

Figure 8: Sink Progression

Once the input and output parameters for the experiment were selected, several tests were performed to determine appropriate levels for the parameters. Each level was varied independently and the resulting part examined. Figures 6 through 8 demonstrate the desired response range. After the parameters that gave this response were determined, the experimental parameter table, shown in Table 2, was assembled. This table consists of the levels used for the first experimental design.

		Levels	
Factor	Code	-1	1
Inject. Press.	A	7.5 ksi	9 ksi
Mold Preheat	B	175 F	212 F
Nozzle Temp.	C	490 F	515 F
Mat'l Preparation	D	Ambient	Oven dried*
Barrel Temp.	E	475 F	495 F
Clamp Force	F	11 tons	15 tons
Cycle Time	G	15 sec	25 sec
Ram Speed	H	8	10

*Held in oven for 2 hours at 200 F

Table 2: Experimental Parameter Levels for DOE1

4 DISCUSSION ON TESTING PROCEDURE

Unfortunately, the resolution on the pre-heat plate is poor (~15°F) as is the feedback. The feedback is essentially the same as that for an oven, the light turns off when the desired temperature is reached. Another problem with the plate is that it just measures temperature at the plate, and not throughout the mold. This could be crucial as there is dramatic heat fluctuation in the mold during a standard cycle. First, molten plastic is injected into it, which causes the mold temperature to rise dramatically. This heat increase is exacerbated by the heat generated due to internal friction in the viscous molten polymer. After the part has cooled, the mold is removed from the press, opened, and exposed to cold air. At this point there is a large surface area exposed, resulting in rapid cooling. A thermocouple, or other temperature sensing device would have improved the accuracy of the mold pre-heat level setting. To combat this problem, we used a standardized pre-heat time of 5 minutes working under the assumption that this was sufficient time for the mold to reach thermal equilibrium in the press. Parts shot from molds that were heated for longer times did not show significant differences from those heated for 5 minutes.

Another factor that was difficult to control was the amount of material in the barrel. We attempted to control this by using the ram return every cycle, and refilling the opening. However, this method is a little inexact and a hopper would be preferable. A variation in the amount of material in the barrel could affect the uniformity of the temperature in the barrel, as well as the cycle time. Cycle time would be affected as the ram would engage the material in a full barrel faster than in a partially empty barrel.

Manual ejection of the mold also added some variability into the process. Several parts were plastically deformed while being removed, and gates and runners were occasionally broken as well. If flatness were an important criterion being considered, manual ejection would have caused a major effect on the response. In addition, manual ejection caused some variability in the cooling time of the part. This is because the mold cannot be removed and opened manually in a consistent amount of time. The addition of automatic ejector pins into the mold could mitigate these problems for future tests.

The biggest problem that was encountered during the experiment was shifting of the upper platen. This is the section of the press that clamps the mold from the top. This shifting was likely due to thermal expansion as the temperature of the press fluctuated. Fluctuations in the mold temperature (as previously discussed), and the accompanying thermal expansion of the mold, exacerbated this problem. Note also that several different temperatures were used during this experiment. The shifting of the upper platen affected the seating of the nozzle, and the clamping of the mold. Occasionally, the mold spontaneously opened during a replicate shot. Similarly, plastic was ejected from the gap between the nozzle and the mold when the nozzle failed to seat properly. Adjustments to the upper platen rectified these problems, but were not accounted for in our DOE. This could account for some of the variability we experienced during our experiments, particularly in the measurement of the part flash.

5 DESIGN OF EXPERIMENTS

Our experimentation was broken up into two designs of experiments. The first experiment (DOE1) concerned itself with identifying the significant variables contributing to part fill. Quantifying flash and sink on under filled parts does not yield meaningful results. For that reason, our second experiment (DOE2) focused on identifying the significant parameters that effected sink and flash while also producing completely filled parts. Both experiments led to the construction of predictive models for both part fill and sink. The following is a brief discussion on the design of our experiments, analysis, and model constructions and verifications.

5.1 DOE1 - Experimentation on Part Fill

Table 2 shows the parameters for DOE1. As you can see testing all combinations of 8 parameters leads to a large run size when considering a full factorial design of experiment (2^8 = 256 test conditions). Ideally, one would like to maximize the amount of information from an experiment in the most efficient manner. Therefore, a fractional factorial design best suits our situation. Fractional factorial design allows one to test more parameters in smaller run sizes. In order to achieve this, a certain degree of confounding between parameter effects occurs. For DOE1, we selected a 2^{8-4}_{IV} design, which yields 16 unique test conditions. Since this is a low run size, we decided to include replications for each test condition in order to generate an estimate of error. This estimate of error allowed us to test the statistical significance of our parameters during analysis. Figure 9 shows the design matrix.

	Basic				Added				Responses			
Run	A	B	C	D	E	F	G	H	y1	y2	···	yk
1	−	−	−	−	−	−	−	−	y11	y12	···	
2	+	−	−	−	−	+	+	+	y21	y22	···	
3	−	+	−	−	+	−	+	+	⋮	⋮		
4	+	+	−	−	+	+	−	−				
5	−	−	+	−	+	+	+	−				
6	+	−	+	−	+	−	−	+				
7	−	+	+	−	−	+	−	+				
8	+	+	+	−	−	−	+	−				
9	−	−	−	+	+	+	−	+				
10	+	−	−	+	+	−	+	−				
11	−	+	−	+	−	+	+	−				
12	+	+	−	+	−	−	−	+				
13	−	−	+	+	−	−	+	+				
14	+	−	+	+	−	+	−	−				
15	−	+	+	+	+	−	−	−				
16	+	+	+	+	+	+	+	+				

Figure 9: DOE1 Matrix

In order to create this fractionated design, a method of coding the appropriate levels for each *added* factor column must be used. Added factors (E,F,G, and H) are ones whose coding patterns depend solely on combinations of *basic* factors (A, B, C, and D). For instance, E = BCD (design generator), meaning that by multiplying out the -'s and +'s in columns B, C, and D together will yield a unique column pattern for E or one

that is orthogonal to the rest of the columns within the design matrix. In that same manner, level assignments for columns F, G, and H can be determined. Figure 10 shows design generators for the added factors.

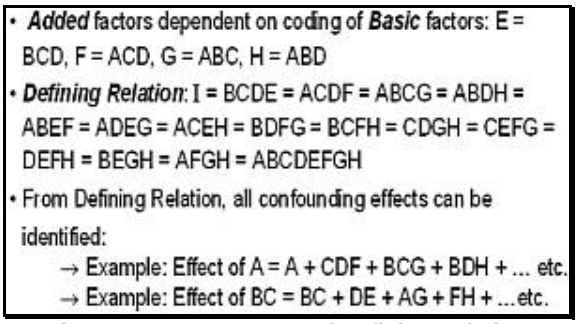

Figure 10: Generators and Defining Relation

At this point, each test condition has the appropriate level assignment for each factor. As mentioned earlier, a degree of confounding between parameters exists within this design when calculating effects. Confounding can be interpreted as the inability to discern a parameter effect from another one. Right away, E = BCD implies that the main effect E cannot be discerned from the three factor interaction effect of BCD. In this case, we made the assumption that three-factor interactions or higher are negligible. Typically, three-factor or higher interactions have a lower probability of occurring or having a large effect in an experiment that is largely mechanically based. Chemical experiments on the other hand may not make the same assumption since chemical reactions of parameters of higher degree occur more frequently. In our case, we must be able to discern our confounded effects. For that reason, a defining relation is developed from multiplying out all combinations of our generators where a parameter times itself equals its identity (for example, A•A = I). One can now determine what main effects or two-factor interactions are confounded with other parameter interactions by simply multiplying the parameter variable by the defining relation as shown in Figure 10.

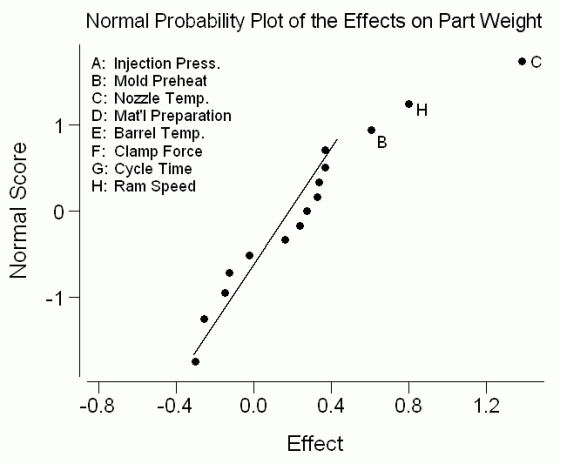

Figure 11: Normal Plot of Effects for DOE1

Results of DOE1 can be seen in Figure 11. The effect estimates on part fill are best seen on a normal probability plot. This is done under the assumption that our observations are not biased nor correlated amongst them selves and that any error existing in our system is normally distributed. For that reason, any effect which does not significantly influence the response should lie along the fitted line whereas any effect which does significantly effect the response will tend to fall off the line. From the plot it appears that nozzle temperature (C), ram speed (H), and mold preheat (B) are significant.

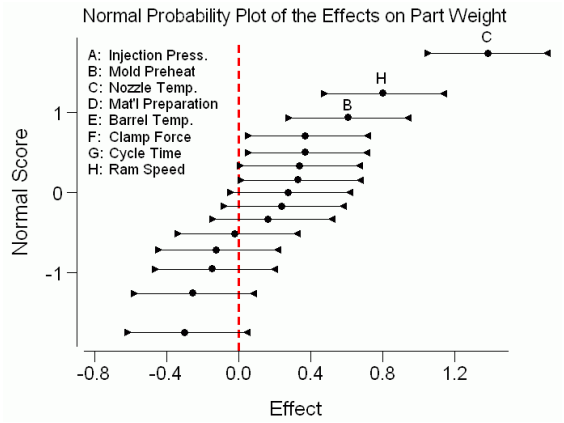

Figure 12: Confidence Intervals of Effects for DOE1

In order to verify the statistical significance of all the effects, confidence intervals (CIs) are constructed using a pooled variance (whereby an effect variance is derived) calculated from our replicates and a *Student's-t* statistic given the total degrees of freedom between our replicates. Figure 12 shows the CIs and their relation to 0.0. If an effect's CI encompasses the value 0.0, statistically the effect is null. Our CIs for B, H, and C do not contain 0.0 so they are statistically significant. Other effects that did not encompass 0.0 but were very close, were neglected. Using the estimates of the average weight and effects, a predictive model can formulated for part fill in grams (1).

$$\hat{y} = 3.778 + 0.303x_B + 0.692x_C + 0.400x_H \quad (1)$$

In addition, residuals can be calculated and plotted (Figure 13) as a first step in model checking. The residuals are calculated using the experimental observations from DOE1.

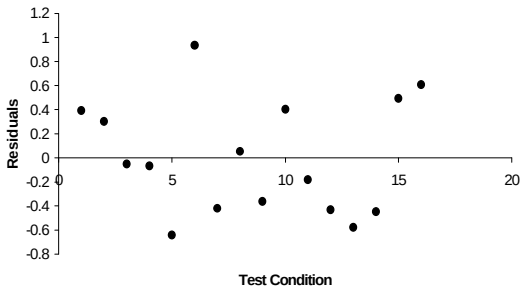

Figure 13: Residuals vs. Test Conditions in DOE1

In order to validate the model in (1), confirmatory tests were run at desired level settings for nozzle temperature, ram speed, and mold preheat temperature. The predicted and experimental results are plotted in Figure 14. The plot shows a relatively good prediction of part fill for the given settings. These confirmatory observations

come from the tests conducted in DOE2 since the conditions of that experiment required nozzle temperature, ram speed, and mold-preheat to be set at constant levels which yield filled parts.

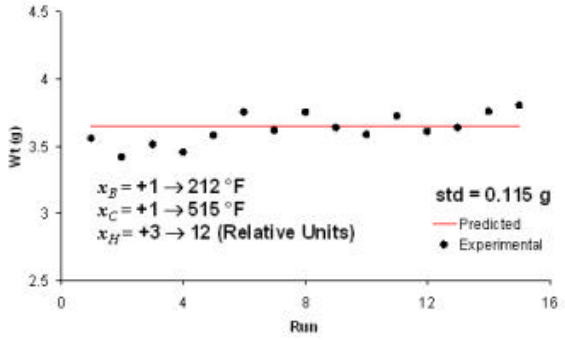

Figure 14: Confirmatory Tests for Part Fill

5.2 DOE2 - Experimentation on Sink and Flash

In order to gather sound data on sink and flash, all observations must be of completely filled parts. Therefore, using the information gathered from DOE1, appropriate level settings for nozzle temperature (C), ram speed (H), and mold-preheat (B) are used and held constant throughout DOE2. As a result, only injection pressure (A), barrel temperature (E), clamp force (F), and cycle time (G) are varied. Material preparation (D) had very little effect on visual defects within the parts in DOE1 that we decided to remove it from DOE2. Figure 15 shows the design matrix for a fractional factorial design of 2_{IV}^{4-1}. The design yields a low run size and allows for efficient replication to be done for each test condition. Again, three-factor or higher interactions are considered negligible for this experiment.

Run	A	G	E	F	y1	y2	...	yk
1	−	−	−	−	y11	y12	...	
2	+	−	−	+	y21	y22	...	
3	−	+	−	+	⋮	⋮		
4	+	+	−	−	⋮	⋮		
5	−	−	+	+	⋮	⋮		
6	+	−	+	−				
7	−	+	+	−				
8	+	+	+	+				

Figure 15: DOE2 Matrix (I=AGEF)

Figure 16 shows a normal plot effects on sink as well as the CIs for the significant effects. The plot indicates that barrel temperature (E), cycle time (G), and injection pressure (A) fall of the line and their CIs do not encompass 0.0. Using the average and effect estimates, a predictive model for sink (2) at the sprue, measured in millimeters, can be constructed.

$$\hat{y} = 0.54 - 0.060x_A - 0.075x_G + 0.281x_E \quad (2)$$

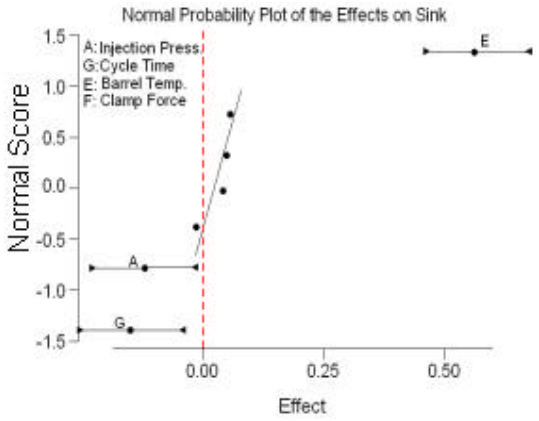

Figure 16: Normal Plot of Effects and CIs for Sink

Confirmatory tests were done to verify the adequacy of the model. Figure 17 shows a plot of experimental and predicted values of sink for the given settings. The experimental results are relatively close to the predicted value.

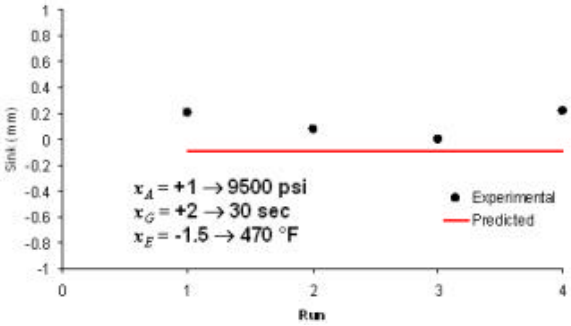

Figure 17: Confirmatory tests for Part Sink

The results of the experiment on our response flash did not yield repeatable data. In Figure 18, a normal plot of effects is shown indicating that cycle time (B) was one of the largest effects contributing to flash. Intuitively, this does not make sense. We were expecting injection pressure (A) and clamping force (D) to be the dominating effects. Their interaction potentially could be active as seen from the plot but before diving into more speculation, the variation must be looked at for each effect.

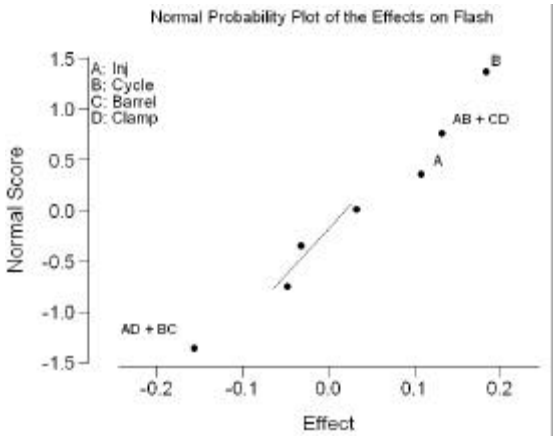

Figure 18: Normal Plot of Effects for Flash

Figure 19 shows the CIs for the significant effects and clearly indicates that these effects are potentially null.

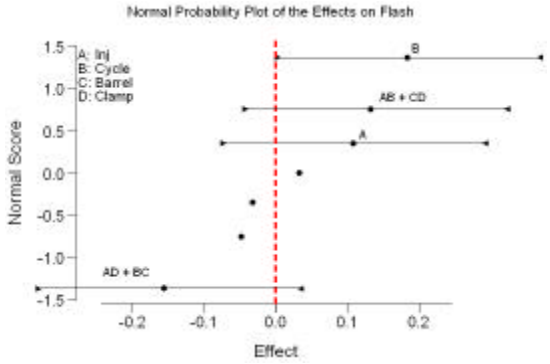

Figure 19: Confidence Intervals for Flash

This a good example of how replicating test conditions can ensure that you are truly getting sound results. In this case, the flash being measured was so small that it could have been masked by the inherent variation within the process. By measuring the weight of the part in quantifying flash, any variation in the way gates were torn off or variation in packing density most likely overshadowed the small amount of flash we were attempting to measure.

6 CONCLUSION

If we look at both DOEs, we see that no two-factor interactions were active and that both predictive models were linear combinations of three main effects. These models may not hold for a different regime of factor level settings. For example, another experiment could be run using the same 8 factors in DOE1 but at different levels. The results from such an experiment may yield strong main effects and two-factor interactions effects.

Also, a significant amount of noise was present within our system, as elaborated in Section 4, yet model (1) was robust enough to still produce completely filled parts. The same was true for part sink (2). Selection of these parameters and level settings led to a robust control of the part fill and sink

Another observation was the strong effect of cycle time on sink . Cycle time's effect on sink may have come out less significant if the sink of the part, rather than the sprue, had been considered. This is because of the fact that once the gate freezes, it is impossible to pack any more material through it. Therefore, any packing time after the freezing of the gate does not affect sink. This problem does not exist at the sprue as it is in direct contact with the molten plastic in the nozzle. However, if we enlarge the gate of a part, we can increase the time it takes for the gate to freeze to correspond to the time required to overpack the part. In this manner, we may be able to reduce the amount of sink in an existing mold.

Finally, the results of our experiments allowed us to construct a saddle surface and sphere from snapping together Triconnector parts. Figures 20 and 21 show the constructions.

Figure 20: Triconnector Saddle Surface

Figure 21: Triconnector Sphere